J. Mol. Biol. (1997) **272**, 398–407

JMB

The High Resolution Crystal Structure of Deoxyhemoglobin S

Daniel J. Harrington[1], Kazuhiko Adachi[2] and William E. Royer, Jr[1]*

[1]*Program in Molecular Medicine, Department of Biochemistry and Molecular Biology, University of Massachusetts Medical School 373 Plantation Street Worcester, MA 01605, USA*

[2]*Division of Hematology The Children's Hospital of Philadelphia, Department of Pediatrics, University of Pennsylvania, School of Medicine, Philadelphia PA 19104, USA*

**Corresponding author*

We have refined the crystal structure of deoxyhemoglobin S (β Glu6 → Val) at 2.05 Å resolution to an *R*-factor of 16.5% (free $R = 21.5\%$) using crystals isomorphous to those originally grown by Wishner and Love. A predominant feature of this crystal form is a double strand of hemoglobin tetramers that has been shown by a variety of techniques to be the fundamental building block of the intracellular sickle cell fiber. The double strand is stabilized by lateral contacts involving the mutant valine interacting with a pocket between the E and F helices on another tetramer. The new structure reveals some marked differences from the previously refined 3.0 Å resolution structure, including several residues in the lateral contact which have shifted by as much as 3.5 Å. The lateral contact includes, in addition to the hydrophobic interactions involving the mutant valine, hydrophilic interactions and bridging water molecules at the periphery of the contact. This structure provides further insights into hemoglobin polymerization and may be useful for the structure-based design of therapeutic agents to treat sickle cell disease.

Keywords: sickle cell disease; hemoglobin S; protein polymerization; molecular disease; protein structure

Introduction

Sickle cell disease results from the mutation of human hemoglobin (HbA) at the sixth position of the β-chain from glutamic acid to valine (Ingram, 1956). Classic studies on the hemoglobin from sickle-cell patients pinpointed the cause of this disease and led to the concept of a ''molecular disease'' (Pauling *et al.*, 1949). This substitution of a hydrophobic residue for an acidic residue results in a drastic decrease in solubility of the protein in the deoxygenated state. Deoxyhemoglobin S (HbS) forms long polymers that distort the normally pliable red blood cells and can hinder passage through the microcirculation. Occlusion of capillaries decreases oxygen supply to surrounding tissues which is believed to be responsible for the clinical manifestations of sickle-cell anemia.

Structural analysis of HbS fibers using single crystal X-ray diffraction, fiber X-ray diffraction and electron microscopy, as well as complementary information from gelation experiments on hemoglobin mutants, has established the basic fiber architecture (Eaton & Hofrichter, 1990). Crystallization of deoxy HbS in low salt at low pH (5.0 to 6.0) produces monoclinic crystals in which hemoglobin molecules are assembled in double strands (Wishner *et al.*, 1975). These ''Wishner-Love'' double strands of HbS are stabilized by axial contacts within each strand and lateral contacts between strands that involve the mutated β Val6 (Wishner *et al.*, 1976). There is strong complementary data suggesting that the double strand with a slight helical twist is the basic building block of intracellular fibers. X-ray fiber diffraction data, from both extracellular gels and sickled erythrocytes, are consistent with a similar arrangement of molecules in the crystal and fiber (Magdoff-Fairchild & Chiu, 1979). Electron microscopy with image reconstruction has revealed that the basic HbS fiber is 210 Å thick and formed from 14-filament strands that associate as half-staggered pairs (Dykes *et al.*, 1979). While some disagreement exists as to the arrangement of the double strands within the HbS fiber (Cretegny & Edelstein, 1993; Watowich *et al.*, 1993), there is broad agreement that the basic building block of the fiber is a Wishner-Love double strand with a slight helical twist. Additional convincing evidence that the crystalline double strand is physiologically relevant comes from copolymerization studies of HbS with naturally occurring variants (Benesch *et al.*, 1982; Nagel

Abbreviations used: HbS, hemoglobin S or sickle cell hemoglobin; HbA, human hemoglobin A; DPG, (2,3)-diphosphoglycerate; RMS, root-mean-square.

0022–2836/97/380398–10 $25.00/0/mb971253

et al., 1980). These experiments show significant changes in the polymerization properties of HbS as a result of altering residues that participate in the crystal double strand contacts. In contrast, most mutations of residues not involved in double-strand contacts do not lead to alterations of the polymerization properties (Eaton & Hofrichter, 1990).

The similarity of the molecular packing within HbS crystals and fibers provides an opportunity to obtain a very detailed understanding of the interactions that trigger polymerization. Previous crystallographic analysis of HbS at 3.0 Å resolution (Padlan & Love, 1985a,b) revealed some details of the interactions between tetramers, including the identification of residues involved, but did not provide precise determination of the stereochemistry of the interfaces, including accurate van der Waals interactions and involvement of water molecules. Here we report the crystal structure of deoxy-HbS at 2.05 Å resolution which reveals important new details of contact formation between HbS tetramers in the physiological double strand.

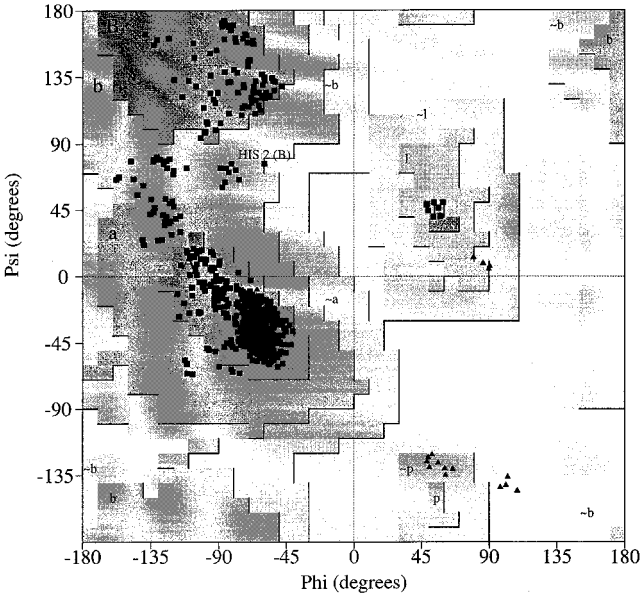

Figure 1. Ramachandran plot generated using PROCHECK (Laskowski *et al.*, 1993). Gray areas represent most favorable regions, and glycine residues are shown as triangles.

Results

The structure of sickle cell hemoglobin has been refined at 2.05 Å resolution to an *R*-factor of 16.5% and a free *R* of 21.5%, with excellent stereochemistry (Table 1). A Ramachandran plot shows no residues in disallowed regions and 93.5% in most favored regions (Figure 1). A Luzzati plot (Luzzati, 1952), generated using the conventional *R*-factor, suggested an upper limit on the overall positional error of roughly 0.22 Å (data not shown), significantly less than the 0.55 Å estimate for the 3.0 Å structure, reflecting the use of higher resolution data in conjunction with improved X-ray structure refinement techniques.

An $F_o - F_c$ omit map of the region including β valine 6 and several other residues in the lateral contact is shown in Figure 2. Electron density maps were also used to check the structure for possible ligand association in either oxygen-bind-

Table 1. Data collection and refinement statistics for the deoxy-HbS structure

Resolution limits (Å)	10–2.05
Total observations	244,980
Unique reflections	72,955
R_{merge} (%)	9.3
Completeness (%)	95.0
No. of reflections used in refinement ($F > 2\sigma$)	64,050
R-factor	0.165
No. of reflections used for *R*-free ($F > 2\sigma$)	7846
R-free	0.215
No. of non-hydrogen atoms:	
Hemoglobin	9105
Solvent	573
R.M.S deviation from ideality:	
Bond lengths (Å)	0.010
Bond angles (°)	1.491
Impropers (°)	1.341
Average temperature factors:	
Protein (Å^2)	19.5
Water (Å^2)	37.9

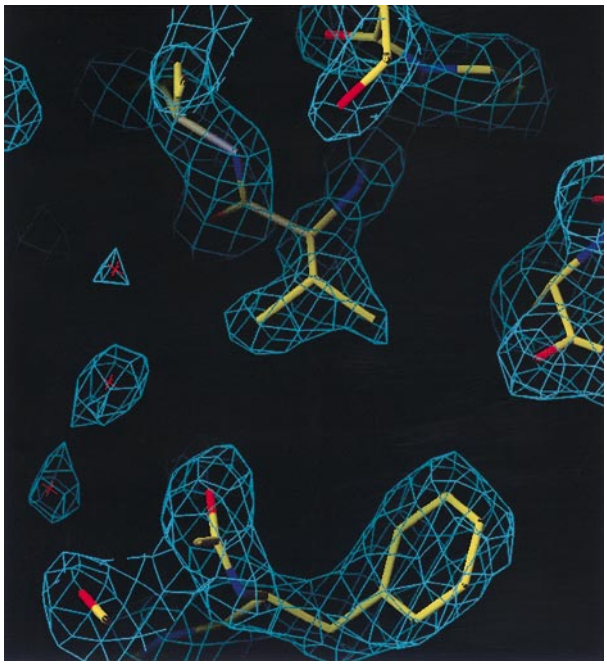

Figure 2. $F_o - F_c$ omit map contoured at 3.0 σ depicting the area immediately surrounding the mutant valine from the $2\beta_2^S$ chain. This residue is involved in lateral contact 1 of the crystal structure. Below and to the right of the centrally-located valine side-chain is $1\beta_1^S$ Phe85, part of the hydrophobic patch from a second tetramer with which $2\beta_2^S$ Val6 interacts. Three water molecules are also visible to the left of the valine side-chain. (Figure generated with O, Jones *et al.*, 1991).

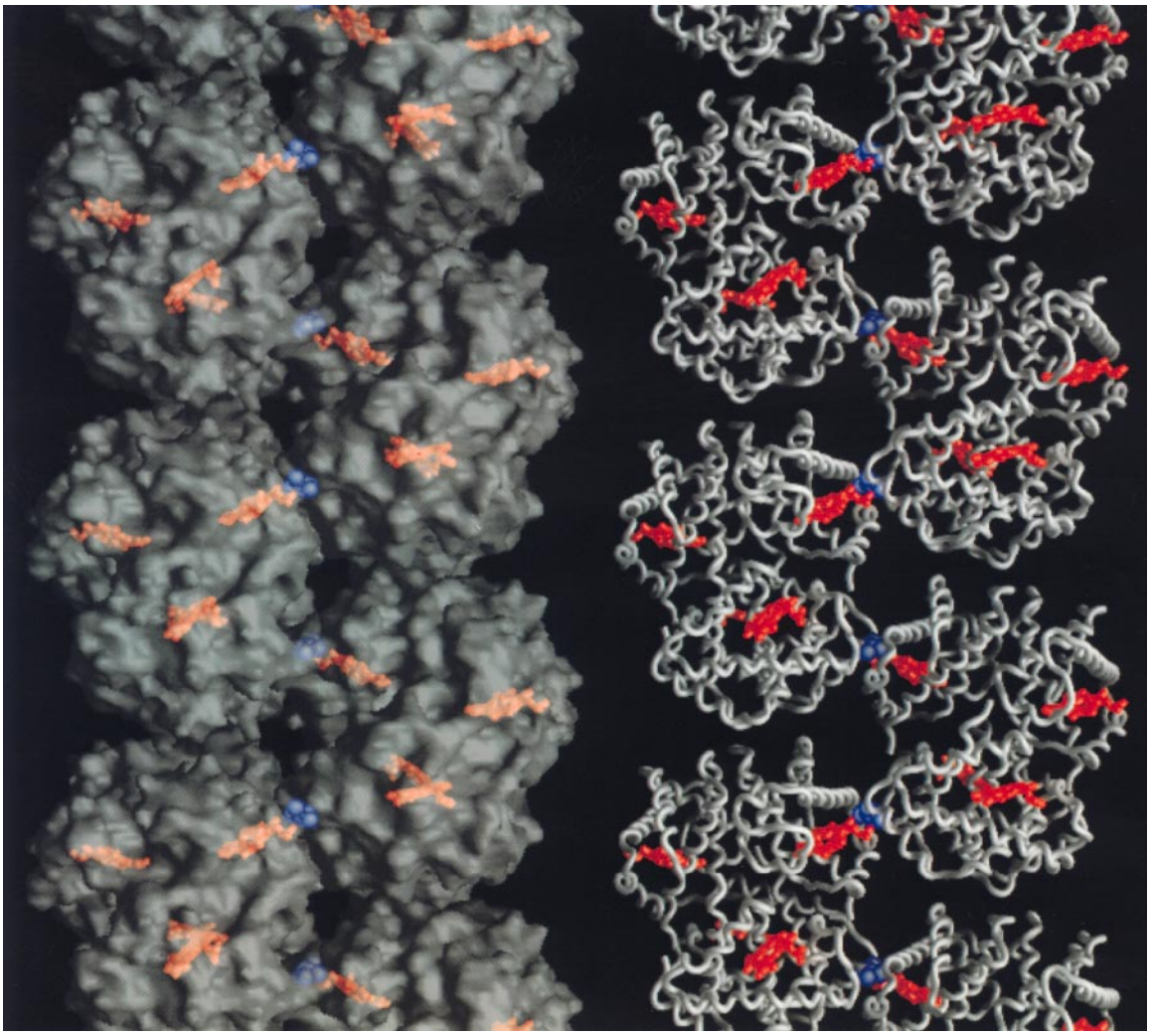

Figure 3. Two depictions of the double strand of hemoglobin molecules found in the crystal. On the left, the strand is shown as a transparent molecular surface, with heme groups colored red, and the mutant valine residues blue. In the representation on the right, the protein backbones are shown as white coils, with the color scheme for heme groups and mutant valine residues remaining the same as the left. The axial contacts are located between molecules within a single strand in the vertical direction. Lateral contacts involving the blue valine residues act to associate the two single strands into the double strand. (Figure generated using GRASP, Nicholls *et al*., 1993).

ing sites or the (2,3)-diphosphoglycerate (DPG)-binding site. No ligands were found in either of these sites, although water molecules were found at positions that can form hydrogen bonds with the distal histidine residues in each α chain heme pocket and in the DPG-binding cleft.

The molecules pack within the crystals as two strands of HbS molecules running parallel to the crystallographic *a* axis. Molecules within each strand contact one another *via* axial contacts, and the two strands are stabilized by lateral contacts involving β Val6 (Figure 3). The asymmetric unit of the crystal contains two tetramers which contact one another *via* a lateral contact. We will adopt the naming convention and designations used previously (Padlan & Love, 1985a,b) to denote individual subunits within this crystal structure. In this scheme, subunits within tetramer 1 or 2 are preceded by a 1 or 2, respectively. The β subunits are assigned according to their contacts, i.e. β^S subunits acting as acceptor pockets for mutant valine residues are designated β_1^S, those acting as valine donors are termed β_2^S (β subunits act as either mutant valine donors or acceptors, but not both). The α chains are named according to their positions relative to the β^S chains. In this manner, all eight crystallographically distinct subunits are assigned unique identifiers.

The individual HbS molecules in the asymmetric unit were compared to each other and to that of deoxy HbA determined at 1.74 Å resolution (Fermi *et al*., 1984). The least-square comparison between α-carbon atoms of tetramer 1 and HbA yielded a root-mean-square (RMS) deviation of 0.56, and tetramer 2 to HbA showed a 0.55 RMS deviation. The RMS deviation for α-carbon atoms between HbS tetramers is 0.32 Å, and for all atoms is 0.65 Å. Among individual subunits, two key areas of structural difference are found when comparing β_1^S subunits with β_2^S subunits. These areas are those

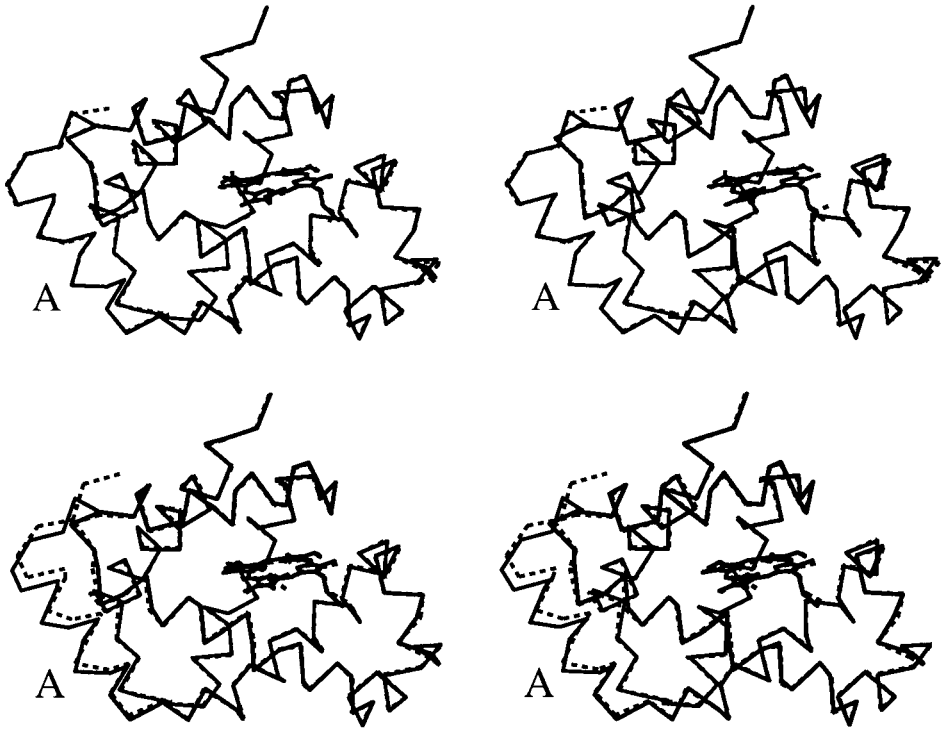

Figure 4. Stereo views showing movement of A helix in $1\beta_2^S$ chain. The upper Figure shows α carbon traces comparing the $1\beta_1^S$ (broken lines) and $2\beta_1^S$ (continuous lines) subunits as superimposed using O (Jones *et al.*, 1991). The bottom Figure depicts the superposition of the donor $1\beta_1^S$ (broken lines) and the acceptor $1\beta_2^S$ (continuous lines) subunits. Heme bonds are also shown in each of the Figures. The A labels the positions of the A helices in each of the Figures. (Figure generated using MOLSCRIPT, Kraulis, 1991).

involved in the lateral contacts, with differences seen in both the donor A helix (which contains the mutant valine), and, to a lesser extent, the acceptor EF corner region. Figure 4 shows these differences, particularly in the area of the A helix, which is displaced to a position closer to the tetramer interior in the β_2^S subunits.

The two crystallographically distinct lateral contacts are shown in Figure 5. The Figures are oriented with a view into the valine-binding EF corner region. Only the valine residues from the β_2^S chains are shown, which are depicted as magenta bonds suspended over the pockets. In both contacts, the geometry of the valine and the residues it contacts in the β_1^S subunit are quite similar. The hydrophobic surface which comprises the valine binding site is shown in yellow directly beneath the valine. This is made up of β_1^S Phe85, β_1^S Leu88, and several heme atoms. Despite the hydrophobicity of this region and the mutant valine, there is a network of water molecules intimately associated with the contact, as shown by the light blue atoms in the Figure. Most of these water molecules are well-ordered, with those displaying lower temperature factors being closely associated with the atoms of the acceptor pocket.

An alternate depiction of the lateral contact is shown in Figure 6. This stereo view shows water molecules and the positions of key residues within the contact. A network of water molecules is present at the bend between the F′ and F helices of the β_1^S subunits. This cluster appears primarily stabilized by hydrogen bonds with main-chain carbonyl oxygen and amide nitrogen atoms at the bend in the acceptor subunit. Additional hydrogen bonds can form with the carbonyl oxygen of β_2^S Val6 and the side-chain of β_2^S Thr123 from the donor subunit. Thus, water molecules form bridging hydrogen bonds between tetramers in the lateral contact. The average *B*-factor of these waters is 28.8 Å^2, with a particularly well-ordered (*B*-factor = 24.9 Å^2) solvent molecule located to accept and donate hydrogen bonds to backbone atoms, effectively continuing the alpha helical hydrogen bond pattern between the F and F′ helices. Table 2 lists all those residues which are involved in pairwise contacts of less than 4.0 Å across the lateral interfaces, along with the corresponding distances in the 3.0 Å structure.

The axial contacts in the HbS crystals are shown in Figure 7. Similar contacts are found in many hemoglobin crystals (Fitzgerald & Love, 1979), and in this crystal structure, there are two crystallographically distinct axial contacts. These are located between tetramers translated vertically (along the crystallographic *a* axis) with respect to one another in the strands as depicted in Figure 3. Therefore, each tetramer is involved in two axial contacts. Table 3 lists distances between residues involved in the axial contacts.

As observed in the 3.0 Å structure, the axial and lateral contacts appear to be the only contacts

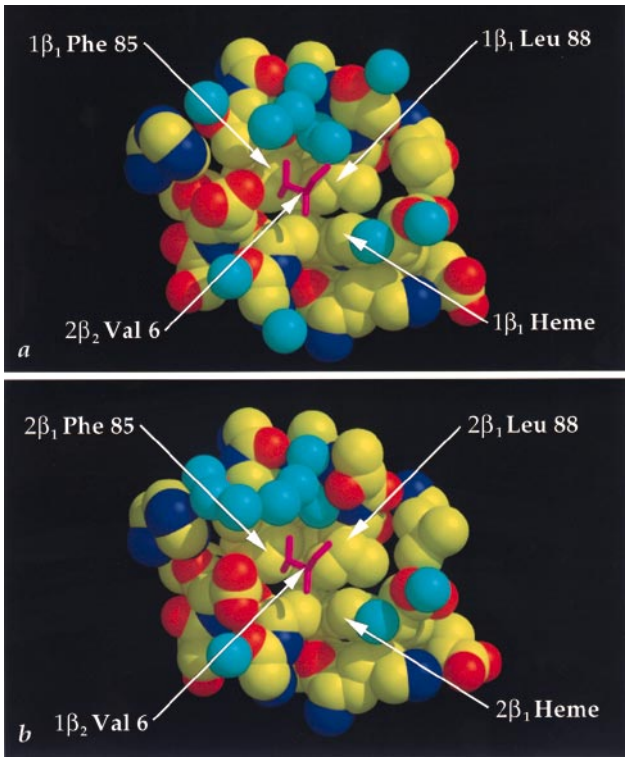

Figure 5. The two crystallographically unique lateral contacts: a, contact 1; b, contact 2. These views show the mutant valine (magenta bonds) positioned in its binding pocket on another tetramer. The atoms of the acceptor pocket are depicted as van der Waals radii, with carbon atoms yellow, oxygen atoms red, nitrogen atoms dark blue, and water molecules light blue. (Figure created using MIDAS, Ferrin *et al.*, 1988).

retained in the crystal which are present in the pathological fiber based on mutational studies. Therefore, an extensive discussion of the residues involved in ''non-physiological'' contacts will not be undertaken here, and we refer the reader to the 3.0 Å structure for a discussion and tabulation of these interactions (Padlan & Love, 1985b).

Discussion

The refinement of the HbS structure using 2.05 Å diffraction data produced a more accurate and complete model. In Figure 8, models of the lateral contact are compared from our analysis and the earlier work at 3.0 Å resolution (Padlan & Love, 1985a). The position of β_1^S Leu88 is of particular interest. In our structure, this residue occupies a position packed in the heme pocket, as in the deoxy HbA structure. The 3.0 Å refinement placed β_1^S Leu88 out of the heme pocket, closer to β Val6, at a position in which we find water molecules. The two independent contacts from our structure are quite similar, in contrast to significant differences seen in the two 3.0 Å structure lateral contacts. This is better illustrated in Table 2, which shows the similarity in the atomic distances between residues in each interface within our structure, and also the differences from the 3.0 Å structure. In our model, both contacts contain roughly the same residues making similar contacts, as expected. This contrasts with the 3.0 Å structure, in which one lateral contact involves far fewer residues than the other.

In the 3.0 Å HbS structure, there were indications that α chain heme pockets were partially

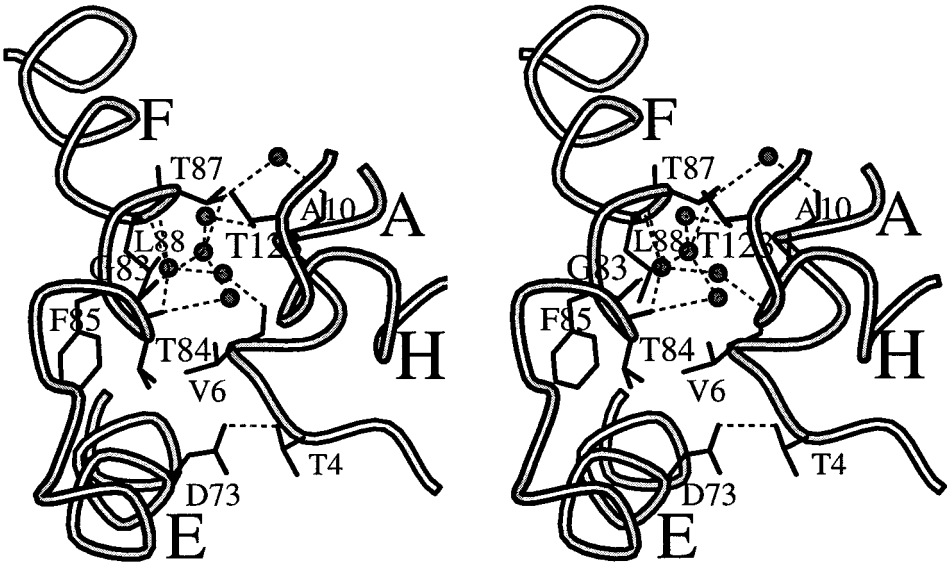

Figure 6. Stereo diagram of the lateral contact. On the right, backbone worms and residues are shown from the $2\beta_2^S$ subunit which contains the mutant valine, and interacts with the $1\beta_1^S$ acceptor pocket as shown on the left. Side-chains which closely associate with the mutant valine or are involved in hydrogen bonds are shown in this Figure. Hydrogen bonds were included if the donor and acceptor atoms were within 3.2 Å of one another according to the program WATERPATH (Steven Sheriff), and these bonds are represented as broken lines. Residues are labeled according to the standard one-letter amino acid code, and the helices of the globin fold are also labeled by capital letters. (Figure generated using MOLSCRIPT, Kraulis, 1991).

Table 2. HbS lateral contacts

Residues	2.0 Å Structure Contact 1 (Å)	2.0 Å Structure Contact 2 (Å)	3.0 Å Structure Contact 1 (Å)	3.0 Å Structure Contact 2 (Å)
β_1^S Lys66 (O)- β_2^S Pro5 (CG)	3.61	3.65[a]	3.32	4.84[a]
β_1^S Gly69 (C)- β_2^S Pro5 (CG)	3.89	3.96	3.78	3.85[a]
β_1^S Ala70 (N)- β_2^S Pro5 (CG)	3.83	3.88	3.23[a]	4.36
β_1^S Ala70 (CB)- β_2^S Val6 (CG2)	3.83	3.82[a]	4.83[a]	3.97[a]
β_1^S Asp73 (OD2)- β_2^S Thr4 (OG1)	3.11	3.01	3.03	4.21[a]
β_1^S Asp73 (OD2)- β_2^S Val6 (CB)	3.10	3.92[a]	2.99	6.32
β_1^S Asp79 (OD2)- α_2 Ser49 (CA)	3.46	3.48	3.27	5.81[a]
β_1^S Asp79 (OD2)- α_2 His50 (N)	2.83	2.88	3.98	7.37
β_1^S Asn80 (CG)- α_2 His50 (CD2)	3.65	3.73[a]	5.71	7.91[a]
β_1^S Gly83 (O)- β_2^S Pro125 (CG)	3.99	4.10	3.46	5.20
β_1^S Thr84 (O)- β_2^S Val6 (CG1)	3.62	3.72	3.23	4.03
β_1^S Phe85 (CE1)- β_2^S Val6 (CG2)	3.95	4.10	4.91[a]	3.65
β_1^S Thr87 (CG2)- β_2^S Ala13 (CB)	3.65	4.63	4.17	3.83
β_1^S Thr87 (OG1)- β_2^S Ala10 (CA)	4.43	3.75	3.99	4.91[a]
β_1^S Thr87 (CG2)- β_2^S Val126 (CG2)	5.98	3.83	5.19[a]	6.06[a]
β_1^S Leu88 (CD2)- β_2^S Ser9 (OG)	3.50	3.36	4.14[a]	3.95
β_1^S Glu90 (OE2)- β_2^S Lys17 (NZ)	5.03	3.49	3.47	5.26
β_1^S Lys95 (NZ)- β_2^S Lys17 (NZ)	3.93	5.78	11.19[a]	9.32[a]

Residues closer than 4.0 Å are included with distances shown only for those atoms making the closest contact for each residue pair, except those designated with [a], for which a closer atom pair is present. Contact 1 and contact 2 refer to the two crystallographically unique lateral contacts. This Table is a tabulation of data derived from the program CONTACTS (CCP4, 1994).

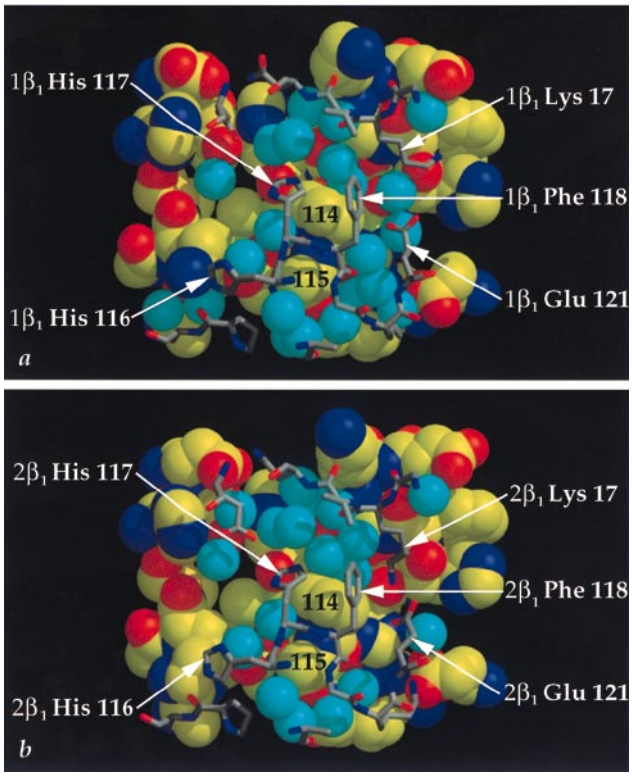

Figure 7. The two crystallographically distinct axial contacts. a, The contact made between symmetry related molecules of the first strand (tetramer 1); b, the second strand (tetramer 2) contact. The space filling models depict atoms of the α_2 and β_2^S subunits, and the bonds decorating this surface model the β_1^S and α_1 loops. The color scheme for the space-filled atoms is as in Figure 6. The bonds are colored gray for carbon, blue for nitrogen, and red for oxygen. (Figure created using MIDAS, Ferrin *et al.*, 1988).

ligated (Padlan & Love, 1985a). Our analysis provides no evidence for oxygen bound to either the α or β chains, but there are water molecules bound to the distal histidine in each of the α chain heme pockets, as seen in HbA (Fermi *et al.*, 1984). The absence of liganded oxygen in our structure could indicate that the anaerobic chamber is more effective than the nitrogen-filled test-tube method (Wishner *et al.*, 1975) at deoxygenating the hemoglobin sample, or it could be an indication of improved phase accuracy resulting from our refinement.

The β chain amino termini have been implicated along with the β His2 residues in binding DPG (Richard *et al.*, 1993). The amino termini of the β^S chains, are not well ordered in our crystal structure showing very high temperature factors with relatively little electron density visible around the first three residues in both $F_o - F_c$ and $2F_o - F_c$ maps. Our crystals, which were grown at a pH between 5.0 and 6.0, were transferred to a pH 7.0 stabilizing solution that contained DPG prior to data collection. Nonetheless, DPG was not seen in our structure. We also crystallized HbS in the presence of DPG with the goal of determining its structural effects on polymerization of HbS. Crystals were grown as described in Materials and Methods, except for the addition of DPG at a 1:1 molar ratio with hemoglobin tetramer. Diffraction analysis, however, indicated that DPG was not bound. It is possible that the crystallization conditions, particularly the low pH (between 5.0 and 6.0), prevent DPG-binding during co-crystallization experiments. DPG exhibits pK_a values of approximately 7.0 and 7.3 (Hobish & Powers, 1983), indicating that it is at least partially protonated during crys-

Table 3. HbS axial contacts

Residues	2.0 Å Structure Strand 1 (Å)	2.0 Å Structure Strand 2 (Å)	3.0 Å Structure Strand 1 (Å)	3.0 Å Structure Strand 2 (Å)
α_1 Pro114 (O)- α_2 Lys16 (NZ)	3.36	5.85	8.07	3.01
α_1 Ala115 (CA)- α_2 Lys16 (CE)	4.81[a]	3.74	8.31[a]	4.10[a]
α_1 Pro114 (CB)- α_2 Glu116 (OE1)	3.71	3.92	4.31[a]	2.92
β_1^S Gly16 (O)- β_2^S Lys120 (NZ)	3.08	4.69[a]	3.25[a]	5.15[a]
β_1^S Gly16 (O)- β_2^S Lys120 (CE)	4.20[a]	3.46	2.86	3.96
β_1^S Lys17 (CG)- β_2^S Phe118 (O)	3.76	3.91	3.86	5.01[a]
β_1^S Lys17 (NZ)- β_2^S His117 (O)	2.86	3.42	5.40[a]	2.92
β_1^S Lys17 (NZ)- β_2^S His116 (O)	6.12[a]	3.42	7.02	4.35
β_1^S Val18 (O)- β_2^S Lys120 (NZ)	3.21	2.93	3.88	4.13[a]
β_1^S Glu22 (OE2)- α_2 His20 (NE2)	3.55	4.85	5.24	5.95[a]
β_1^S His117 (O)- α_2 Pro114 (CG)	3.36	3.47	3.78	3.02
β_1^S His117 (O)- α_2 Ala115 (CB)	3.37	3.26	3.35	6.40[a]
β_1^S Phe118 (C)- α_2 Ala115 (CB)	3.82	3.69	3.09	5.28
β_1^S Phe118 (CD1)- α_2 Pro114 (CG)	3.92	3.55	4.93[a]	6.02[a]
β_1^S Gly119 (N)- α_2 Ala115 (CB)	3.78	3.63	3.18	5.69[a]
β_1^S Glu121 (OE2)- α_2 Pro114 (CB)	3.71	3.79	4.63[a]	3.71

Residues closer than 4.0 Å are included with distances shown only for those atoms making the closest contact for each residue pair, except those designated with [a], for which a closer atom pair is present. Strand 1 and strand 2 refer to the two crystallographically unique lateral contacts formed by tetramers 1 and 2 respectively. This Table is a tabulation of data derived from the program CONTACTS (CCP4, 1994).

tallization below pH 6.0. The inability of DPG to bind in crystals stabilized at pH 7.0 suggests the crystal lattice may sterically prevent binding.

A systematic analysis of the individual subunits of HbS and HbA was undertaken to determine if polymerization perturbs subunit structure. The α chains showed no significant differences among the four crystallographically unique chains (data not shown). The comparisons of the $1\beta_1^S$ with $2\beta_1^S$ and $1\beta_2^S$ with $2\beta_2^S$ chains yielded very little difference between atomic positions, while unlike chains (i.e. $1\beta_1^S$ and $1\beta_2^S$) showed significant differences. These changes are primarily confined to areas involved in the lateral contact, with changes seen in both the donor (β_2^S) and acceptor (β_1^S) subunits. The hinge-like movement of the A helices and the subtle changes in the positions of residues in the acceptor pocket demonstrate that plasticity in both the donor and acceptor chains of the lateral contact facilitates binding.

The acceptor pocket effectively buries the mutant valine in the lateral contact, removing it from most solvent interaction. As seen in Table 2, the mutant valine contacts atoms from four different residues, more than any other residue in this interface. However, the distances between the mutant valine and

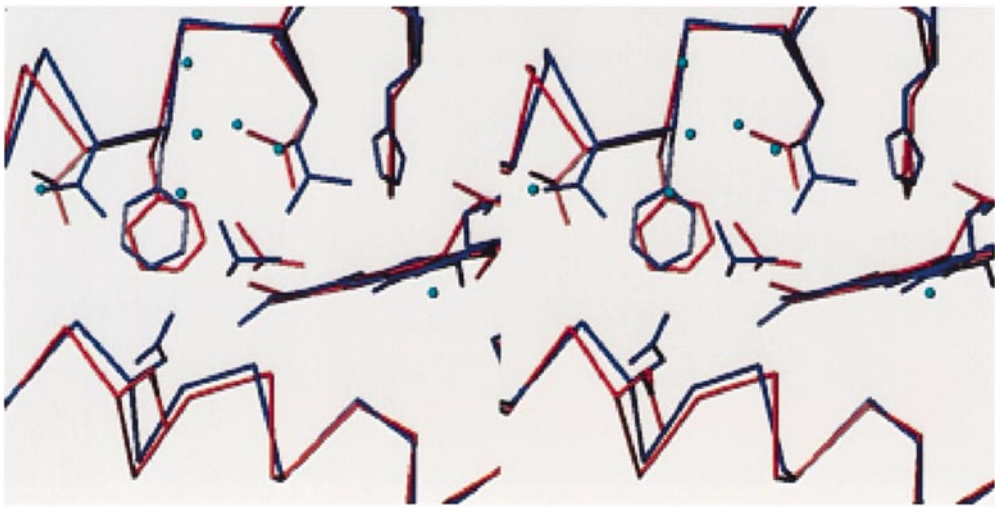

Figure 8. Stereo diagram comparing the residues of the 3.0 Å structure of HbS to the 2.05 Å structure in the area of the lateral contact. The 2.05 Å structure is depicted in blue, with water molecules visible as small light blue spheres. The red bonds represent the 3.0 Å structure. The β_2^S Val6 side-chains are depicted above the acceptor pocket, with their γ carbon atoms facing left in this view. Note the large differences in position of β_1^S Leu88 between the two structures, as shown just above and to the right of β_2^S Val6. The molecules were aligned and displayed using O, (Jones *et al.*, 1991).

the hydrophobic residues of the acceptor pocket indicate that only a few atom pairs are in close van der Waals contact. In addition to buried hydrophobic regions, ordered water molecules near the valine side-chain provide bridging hydrogen bonds across the lateral contact. These water molecules are clustered in the bend between the F′ and F helix, which is found in mammalian but not invertebrate and primitive vertebrate hemoglobins (see Figure 2, Aronson *et al*., 1994). This hydrated bend appears essential for formation of the observed lateral contact. The presence of water molecules illustrates that, although the core of the lateral contact is hydrophobic, extensive hydrophilic interactions also occur between tetramers.

The lateral contact also involves an interaction between the acceptor pocket β chain (β_1^S) and the α_2 chain from the donor tetramer. This is seen in Table 2 as contacts between β_1^S Asp79 and β_1^S Asn80 with α_2 Ser49 and α_2 His50. The interaction is more extensive in our structure than in the 3.0 Å structure, and the association of β_1^S Asn80 with α_2 His50 is only seen in our structure. Studies of hemoglobin mutants (Hemoglobin G Szuhu (β_1^S Asn80 → Lys)) polymerized with HbS show the β_1^S 80 position to be important in the polymerization process (Nagel *et al*., 1980).

The other physiologically relevant interfaces in the crystal are the axial contacts. These involve molecular interfaces between tetramers translated one unit cell along the *a* axis (vertical in Figure 3). The residues involved in this interface are indicated in Table 3. The interface is made up of α_2 AB, α_2 GH, and the β_2^S GH corners from the lower tetramer, and β_1^S AB, β_1^S GH, and the α_1 GH corners from the upper tetramer. The contact is dominated by non-polar interactions involving α_2 Pro114 and α_2 Ala115 of one tetramer interacting with β_1^S His116, β_1^S His117, and β_1^S Phe118 of a second tetramer. The β, γ, and δ carbon atoms of α_2 Pro114 form a bulge on the protein surface which is covered by a small pocket formed between the side-chains of β_1^S His117 and β_1^S Phe118 (Figure 5). In this contact, β_1^S Lys17 and β_1^S Glu121 are examples of several disordered residues on the periphery which display different conformations in the two interfaces. Water molecules also show some variability, particularly those located away from the core hydrophobic interaction.

Recent studies using recombinant hemoglobin have shown that the β_1^S 95 position is important for promotion of polymerization (Himanen *et al*., 1995). Our structure has β_1^S Lys95 placed so that its terminal amino group is close (3.93 Å) to the terminal amino group of β_2^S Lys17 from the donor tetramer in one of the lateral contacts. Both chains, however, are disordered (temperature factors for γ, δ, and ζ atoms greater than 35 Å^2), and such interactions would be unfavorable. Nor is there any involvement of this residue in either tetramer in any non-physiological lattice contacts. This is consistent with the interpretation that β_1^S Lys95 is involved in inter-double strand contacts (Cretegny & Edelstein, 1993; Watowich *et al*., 1993).

The double strands found in the crystal are straight, while electron microscopic investigations indicate that the double strands have a slight helical twist in fibers (Eaton & Hofrichter, 1990). This twist is very subtle, with ten tetramer pairs required to facilitate one quarter of a helical turn (Edelstein, 1981). Padlan & Love (1985b) proposed that differences in the extent of interaction in the two distinct lateral contacts could account for the helical twist. In the refined structure, however, the two crystallographically unique lateral contacts are quite similar. We believe that accomodation by residues in the periphery of the axial and lateral contacts would permit twisted strand formation, while the core hydrophobic interactions of these contacts would remain basically unchanged. Our refined structure provides an initial model to test this hypothesis with site-directed mutagenesis and molecular modelling.

We have determined a high resolution model of sickle cell hemoglobin from a physiologically relevant crystal form. Our structural analysis shows key differences from the lower resolution model, most notably in the lateral contacts. The accurate positioning of side-chains combined with the placement of solvent permits a renewed effort for design of inhibitors of HbS polymerization. This accurate model will be useful for structure-based mutational studies aimed at further elucidating the contributions of individual amino acids in the polymerization process.

Materials and Methods

Preparation of HbS

HbS was obtained from the discarded blood of patients with sickle cell disease who received exchange transfusions. Heparinized red cells were washed with a 0.9% (w/v) saline solution. Packed cells were hemolyzed in five volumes of 5 mM potassium phosphate buffer (pH 7.4), containing 0.5 mM EDTA. After removing stroma, HbS in the CO form was purified using a DEAE Sephadex column by gradient elution from 40 mM Tris-HCl (pH 8.3) to 40 mM Tris-HCl (pH 7.3) as described elsewhere (Adachi & Asakura, 1979).

Crystallization

Crystals were grown by the method published previously (Wishner *et al*., 1976), with several modifications. HbS was suspended in 30 mM phosphate buffer (pH 7.0), decarboxylated and deoxygenated, then concentrated to approximately 120 mg/ml. This sample was then transferred into an anaerobic chamber (Anaerobe Systems, Santa Clara, CA, U.S.A.), a few grains of sodium dithionite added, and a visible spectrum taken to confirm deoxygenation just prior to the crystallization setup. Crystallization was carried out using the procedure of Wishner *et al*. (1976), except for a decrease in volumes used. In one to two days, the samples polymerized into the distinctive HbS gel. Crystals formed from the gelled HbS after approximately

12 days, but were allowed to grow for up to three months. As with those grown by Wishner *et al*. (1976), crystals grew twinned at pH 5.0 to 6.0, and had to be transferred to a stabilizing solution (pH 7.0) and cut prior to mounting. All crystal manipulations including buffer changes and crystal cutting were performed in the anaerobic chamber.

Data collection

Diffraction data were measured on a RAXIS-IIC imaging plate system mounted on a Rigaku RU-200 rotating anode generator (Molecular Structure Corporation, The Woodlands, TX, U.S.A.), operating at 50 kV, 100 mA. Crystals were mounted in 2 mm diameter glass capillaries (Charles Supper Company, Natick, MA, U.S.A.) in the anaerobic chamber, and sealed with epoxy cement. The crystals exhibited diffraction to Bragg spacings corresponding to 2.0 Å resolution, and diffraction data were collected from three crystals. These showed the symmetry of space group $P2_1$, with cell constants $a = 52.93$ Å, $b = 185.68$ Å, $c = 63.34$ Å, and $\beta = 92.74^\circ$. All three crystals used for this study grew in the same culture tube which contained 10 µl of protein (120 mg/ml), 5 µl citrate buffer (pH 4.0), and 4 µl of 33% PEG 8000. Data were collected from the first crystal mounted with its *b* axis perpendicular to the spindle axis. The second and third were mounted such that the *b* axis was roughly parallel to the spindle axis to allow a larger oscillation angle to be used (3.0 degrees), which lowered the *R*-merge of the scaled data. The data were processed and scaled with DENZO and SCALEPACK, respectively (Otwinowski, 1993). The intensity data were merged using seven frames from the first crystal, 18 from the second, and 47 from the third, yielding 244,989 total observations. From these data, 72,955 unique reflections were obtained, which constitutes 95.0% of predicted data to 2.05 Å, with an *R*-merge of 9.3%.

Refinement

Using the data collected to 2.05 Å, and the 3.0 Å structure (Padlan & Love, 1985a) as the initial model, simulated annealing protocols were performed using XPLOR (Brünger, 1992b). A test set containing 10% of the diffraction data was reserved for determination of a free *R*-factor (Brünger, 1992a), which was used throughout the entire refinement process. In the first round, the two tetramers were restrained by non-crystallographic symmetry (NCS); in the second round, all NCS restraints were lifted. After these molecular dynamics minimizations, the free *R*-factor had dropped from 37.9 to 27.1%, while the conventional *R* dropped from 37.8 to 21.2%. Five shells of water molecules were then added using the programs PEAKS and LOCATE, written by Wayne Hendrickson (Columbia University), and refined using positional refinement and individual *B*-factor refinement, but no simulated annealing. Water molecules were located as peaks with density greater than 3.0 σ in $F_o - F_c$ maps, and greater than 1.0 σ in $2F_o - F_c$ maps, which were also stereochemically reasonable. At each step of the refinement process, the free *R*-factor was monitored, and structures for which this value decreased were kept. After each water shell addition, the structure was analyzed using the molecular visualization program O (Jones *et al*., 1991) to check for agreement with $2F_o - F_c$ and $F_o - F_c$ maps. A bulk solvent correction was applied to the final structure. The atomic coordinates and structure factors have been deposited in the Protein Data Bank under the accession number 2HBS.

The program WATERPATH, written by Steve Sheriff (Bristol-Meyers Squibb Institute), was used to check the lateral and the axial interfaces for bridging water molecules, and these water molecules were included in the Figures.

Acknowledgments

We thank Drs Wayne Hendrickson and Steven Sheriff for computer programs, and Drs Warner Love and Eduardo Padlan for helpful discussions. This work was supported by a Grant-in-Aid from the American Heart Association (W.E.R.), National Institutes of Health Grant P60 HL38632 (K.A.), a March of Dimes Birth Defects Foundation Grant (K.A.), and was carried out during the tenure of an Established Investigatorship from the American Heart Association to W.E.R.

References

Adachi, K. & Asakura, T. (1979). Nucleation-controlled aggregation of deoxyhemoglobin S. *J. Biol. Chem.* **254(16)**, 7765–7771.

Aronson, H.-E. G., Royer, W. E., Jr & Hendrickson, W. A. (1994). Quantification of tertiary structural conservation despite primary sequence drift in the globin fold. *Protein Sci.* **3**, 1706–1711.

Benesch, R. E., Kwong, S. & Benesch, R. (1982). The effects of alpha chain mutations cis and trans to the β6 mutation on the polymerization of sickle cell hemoglobin. *Nature,* **299**, 231–234.

Brünger, A. T. (1992a). Free *R* value: a novel statistical quantity for assessing the accuracy of crystal structures. *Nature,* **355**, 471–475.

Brünger, A. T. (1992b). *X-PLOR* (*Version 3.1*), Yale University Press, New Haven, CT, USA.

Collaborative Computational Project No. 4, (1994). The CCP4 Suite: The SERC (UK) Collaborative Programs for Protein Crystallography distributed from Daresbury Laboratory, Warrington, WA4 4AD, UK. *Acta Crystallog. sect. D,* **50**, 760–763.

Cretegny, I. & Edelstein, S. J. (1993). Double strand packing in hemoglobin S fibers. *J. Mol. Biol.* **230**, 733–738.

Dykes, G. W., Crepeau, R. H. & Edelstein, S. J. (1979). Three-dimensional reconstruction of 14-filament fibers of hemoglobin S. *J. Mol. Biol.* **130**, 451–472.

Eaton, W. A. & Hofrichter, J. (1990). Sickle cell hemoglobin polymerization. *Advan. Protein Chem.* **40**, 263–279.

Edelstein, S. J. (1981). Molecular topology in crystals and fibers of hemoglobin S. *J. Mol. Biol.* **150**, 557–575.

Fermi, G., Perutz, M. F., Shaanan, B. & Fourme, R. (1984). The crystal structure of human deoxyhaemoglobin at 1.74 Å resolution. *J. Mol. Biol.* **175**, 159–174.

Ferrin, T. E., Huang, C. C., Jarvis, L. E. & Langridge, R. (1988). The MIDAS display system. *J. Mol. Graphics,* **6**, 13–27.

Fitzgerald, P. M. D. & Love, W. E. (1979). Structure of deoxyhemoglobin C (beta six glu → lys) in two crystal forms. *J. Mol. Biol.* **132**, 603–619.

Himanen, J.-P., Schneider, K., Chait, B. & Manning, J. M. (1995). Participation and strength of interaction of lysine 95(β) in the polymerization of hemoglobin S as determined by its site-directed substitution to isoleucine. *J. Biol. Chem.* **270**, 13885–13891.

Hobish, M. K. & Powers, D. A. (1983). The binding of physiologically significant protons to 2,3-diphosphoglycerate. *Biophys. Chem.* **18**, 407–411.

Ingram, V. M. (1956). A specific chemical difference between the globins of normal human and sickle-cell anemia hemoglobin. *Nature,* **178**, 792–794.

Jones, T. A., Zou, J.-Y., Cowan, S. W. & Kjeldgaard, M. (1991). Improved methods for building protein models in electron density maps and the location of errors in these models. *Acta Crystallog. sect. A,* **47**, 110–119.

Kraulis, P. J. (1991). MOLSCRIPT: a program to produce both detailed and schematic plots of protein structures. *J. Appl. Crystallog.* **24**, 946–950.

Laskowski, R. A., MacArthur, M. W., Moss, D. S. & Thornon, J. M. (1993). PROCHECK: a program to check the stereochemical quality of protein structures. *J. Appl. Crystallog.* **26**, 283–291.

Luzzati, P. V. (1952). Traitment stastique des erreurs dans ladetermination des structures cristalline. *Acta Crystallog.* **5**, 802–810.

Magdoff-Fairchild, B. & Chiu, C. C. (1979). X-ray diffraction studies of fibers and crystals of deoxygenated sickle-cell hemoglobin. *Proc. Natl Acad. Sci. USA,* **76**, 223–226.

Nagel, R. L., Johnson, J., Bookchin, R. M., Garel, M. C., Rosa, J., Schiliro, G., Wajcman, H., Labie, D., Moo-Penn, W. & Castro, O. (1980). β Chain contact sites in the hemoglobin S polymer. *Nature,* **283**, 832–834.

Nicholls, A., Bharadwaj, R. & Honig, B. (1993). GRASP: a graphical representation and analysis of surface properties. *Biophys. J.* **64**, A166.

Otwinowski, Z. (1993). Oscillation Data Reduction Program. In *Proceedings of the CCP4 Study Weekend: Data Collection and Processing* (Sawyer, L., Isaacs, N. & Bailey, S., eds), SERC Daresbury Laboratory, Warrington, UK.

Padlan, E. A. & Love, W. E. (1985a). Refined crystal structure of deoxyhemoglobin S: I. Restrained least-squares refinement at 3.0 Å resolution. *J. Biol. Chem.* **260**, 8272–8279.

Padlan, E. A. & Love, W. E. (1985b). Refined crystal structure of deoxyhemoglobin S: II Molecular interactions in the crystal. *J. Biol. Chem.* **260**, 8280–8291.

Pauling, L., Itano, H. A., Singer, S. J. & Wells, I. C. (1949). Sickle cell anemia, a molecular disease. *Science,* **110**, 543–548.

Richard, V., Dodson, G. G. & Mauguen, Y. (1993). Human deoxyhaemoglobin-2,3-diphosphoglycerate complex: low-salt structure at 2.5 Å resolution. *J. Mol. Biol.* **233**, 270–274.

Watowich, S. J., Gross, L. J. & Josephs, R. (1993). Analysis of the intermolecular contacts within sickle hemoglobin fibers: effect of site-specific substitutions, fiber pitch and double-strand disorder. *J. Struct. Biol.* **111**, 161–179.

Wishner, B. C., Ward, K. B., Lattman, E. E. & Love, W. E. (1975). Crystal structure of sickle-cell deoxy-hemoglobin at 5 Å resolution. *J. Mol. Biol.* **98**, 179–194.

Wishner, B. C., Hanson, J. C., Ringle, W. M. & Love, W. E. (1976). Crystal structure of sickle-cell deoxy hemoglobin. In *Proceedings of the Symposium on Molecular and Cellular Aspects of Sickle Cell Disease* (Hercules, J. I., Cottam, G. L., Waterman, M. R. & Schechter, A. N., eds), pp. 1–31, DHEW Publ. No. (NIH) 76-1003, Bethesda, MD.

Edited by K. Nagai

(Received 27 March 1997; received in revised form 25 June 1997; accepted 4 July 1997)